0026-895X/07/7103-676–685$20.00
MOLECULAR PHARMACOLOGY
Vol. 71, No. 3
28225/3178466
Mol Pharmacol 71:676–685, 2007
Printed in U.S.A.

Isolation and Structure-Activity of μ-Conotoxin TIIIA, A Potent Inhibitor of Tetrodotoxin-Sensitive Voltage-Gated Sodium Channels

Richard J. Lewis, Christina I. Schroeder, Jenny Ekberg, Katherine J. Nielsen, Marion Loughnan, Linda Thomas, Denise A. Adams, Roger Drinkwater, David J. Adams, and Paul F. Alewood

Institute for Molecular Bioscience, the University of Queensland, St. Lucia, Queensland, Australia (R.J.L., C.I.S., J.E., K.J.N., M.L., L.T., D.A.A., P.F.A.); School of Biomedical Sciences, the University of Queensland, St. Lucia, Queensland, Australia (R.J.L., J.E., D.J.A.); and Xenome Ltd., Indooroopilly, Queensland, Australia (K.N., R.D.).

Received June 22, 2006; accepted November 16, 2006

ABSTRACT

μ-Conotoxins are three-loop peptides produced by cone snails to inhibit voltage-gated sodium channels during prey capture. Using polymerase chain reaction techniques, we identified a gene sequence from the venom duct of *Conus tulipa* encoding a new μ-conotoxin-TIIIA (TIIIA). A ^{125}I-TIIIA binding assay was established to isolate native TIIIA from the crude venom of *Conus striatus.* The isolated peptide had three post-translational modifications, including two hydroxyproline residues and C-terminal amidation, and <35% homology to other μ-conotoxins. TIIIA potently displaced [^{3}H]saxitoxin and ^{125}I-TIIIA from rat brain ($Na_v1.2$) and skeletal muscle ($Na_v1.4$) membranes. Alanine and glutamine scans of TIIIA revealed several residues, including Arg14, that were critical for high-affinity binding to tetrodotoxin (TTX)-sensitive Na^+ channels. We were surprised to find that [E15A]TIIIA had a 10-fold higher affinity than TIIIA for TTX-sensitive sodium channels (IC_{50}, 15 vs. 148 pM at rat brain membrane). TIIIA was selective for $Na_v1.2$ and -1.4 over $Na_v1.3$, -1.5, -1.7, and -1.8 expressed in *Xenopus laevis* oocytes and had no effect on rat dorsal root ganglion neuron Na^+ current. ^{1}H NMR studies revealed that TIIIA adopted a single conformation in solution that was similar to the major conformation described previously for μ-conotoxin PIIIA. TIIIA and analogs provide new biochemical probes as well as insights into the structure-activity of μ-conotoxins.

Voltage-gated sodium channels (VGSCs) control the influx of sodium ions responsible for action potentials in excitable cells (Catterall, 2000). VGSC subtypes are classified $Na_v1.1$ to $Na_v1.9$ according to α-subunit sequence (Catterall et al., 2005). They are further characterized by their sensitivity to TTX, a toxin initially isolated from the Pacific puffer fish. TTX-sensitive (TTX-S) subtypes are inhibited by TTX in the nanomolar range and include the neuronal subtypes $Na_v1.1$, -1.2, -1.3, -1.6. and -1.7 and the skeletal muscle $Na_v1.4$ (Goldin et al., 2000). The VGSC $Na_v1.5$, -1.8, and -1.9 are inhibited by TTX in the micromolar range and classified as TTX-resistant (TTX-R).

VGSC channelopathies underlie a number of neuromuscular and cardiovascular diseases including long QT syndrome and epilepsy (George, 2005). Certain VGSC subtypes, such as $Na_v1.3$, -1.7, -1.8, and -1.9 are likely to be involved in pain pathways (Wood et al., 2004) and represent attractive targets for the development of pain therapeutics. The general paucity of selective VGSC blockers remains a major obstacle to the development of drugs at these targets; currently available modulators cause side effects as a consequence of actions at multiple subtypes. Inhibitors of VGSCs with greater selectivity may allow the development of improved therapeutics.

Six toxin binding sites (sites 1−6) and a local anesthetic site have been identified on VGSCs (Catterall et al., 2005). At

This work was supported by Australian National Health and Medical Research Council (NHMRC) Program grant 351446, a Grant for Industry Research and Development from AusIndustry, and NHMRC Project grant 210307.

Article, publication date, and citation information can be found at http://molpharm.aspetjournals.org.

doi:10.1124/mol.106.028225.

ABBREVIATIONS: VGSC, voltage-gated sodium channel; TTX, tetrodotoxin; TTX-S, TTX-sensitive; TTX-R, TTX-resistant; STX, saxitoxin; SAR, structure-activity relationship; GIIIA, μ-conotoxin-GIIIA; GIIIB, μ-conotoxin-GIIIB; PIIIA, μ-conotoxin-PIIIA; SmIIIA, μ-conotoxin-SmIIIA; TIIIA, μ-conotoxin-TIIIA; 3D, three-dimensional; PCR, polymerase chain reaction; RP, reversed-phase; HPLC, high-performance liquid chromatography; MS, mass spectrometry; DRG, dorsal root ganglia; NOESY, nuclear Overhauser effect spectroscopy; COSY, correlation spectroscopy; RMSD, root mean square deviation; NOE, nuclear Overhauser effect; PBD, Protein Data Bank.

site 1, two classes of Na^+ channel inhibitors have been identified that act competitively in the outer pore region of the α-subunit of TTX-S VGSCs (Cestele and Catterall, 2000); the three-loop peptidic μ-conotoxins from the venom of fish-hunting cone snails and the guanidinium-containing TTX and saxitoxin (STX) from puffer fish, bacteria, and dinoflagellates. The sequences of μ-conotoxins identified so far are provided in Table 1. Each of these has six cysteines forming three disulfide bridges in the 1-4, 2-5, 3-6 configuration. Of these, μ-conotoxin-GIIIA (GIIIA), μ-conotoxin-GIIIB (GIIIB), and μ-conotoxin-GIIIC inhibit skeletal muscle VGSCs and μ-conotoxin-PIIIA (PIIIA) nonselectively inhibits nerve and muscle TTX-S Na^+ channels (Shon et al., 1998; Safo et al., 2000; Nielsen et al., 2002), whereas μ-conotoxin-SmIIIA (SmIIIA), μ-conotoxin-SIIIA, and μ-conotoxin-KIIIA inhibit the amphibian TTX-R Na^+ channel (West et al., 2002; Keizer et al., 2003; Bulaj et al., 2005). The interesting diversity of activity displayed by μ-conotoxins makes them important tools for probing the various VGSC subtypes.

Previous structure-activity relationship (SAR) studies have shown that all μ-conotoxins possess either a conserved arginine (Chahine et al., 1995; Chang et al., 1998) or a conserved lysine in loop 2 (Bulaj et al., 2005) that is critical for high-affinity block. NMR structures of GIIIA (Lancelin et al., 1991), GIIIB (Hill et al., 1996), PIIIA (Nielsen et al., 2002), and SmIIIA (Keizer et al., 2003) reveal that this basic residue is highly exposed, allowing it to enter into the mouth of the channel, where it overlaps with the TTX binding site. In early studies, the 3D structure of GIIIA was used as a probe to investigate the dimensions of the outer vestibule of the VGSC (French et al., 1996). However, recent studies revealed the existence of multiple conformation of PIIIA in solution, with the major conformation differing from the major conformation of GIIIA and GIIIB. The presence of multiple conformations makes it difficult to identify the true binding conformation of μ-conotoxins.

Here, we report the isolation and characterization of μ-conotoxin TIIIA identified from a *Conus tulipa* gene sequence. ^1H NMR studies revealed that TIIIA exists as a single, well defined conformation in solution that is equivalent to the major conformation of PIIIA (Nielsen et al., 2002) but not that of GIIIA and GIIIB (Hill et al., 1996). Structure-activity studies examining peptides consisting of alanine and glutamine analogs of TIIIA revealed residues important for activity at both neuronal ($Na_v1.2$) and muscle ($Na_v1.4$) VGSC subtypes. A comparison of the three-dimensional structures of TIIIA, PIIIA, GIIIB, and SmIIIA indicate a common set of structural features that are important for μ-conotoxin binding to VGSCs.

TABLE 1

μ-Conotoxin sequences and connectivity (cysteines 1-4, 2-5, 3-6 are paired)

Peptide	Sequence	Reference
TIIIA	RHGCCKGOKGCSSRECRO-QHCC*	This article
GIIIA	RDCCTOOKKCKDRQCKO-QRCCA*	Cruz et al., 1985
GIIIB	RDCCTOORKCKDRRCKO-MKCCA*	Cruz et al., 1985
GIIIC	RDCCTOOKKCKDRRCKO-LKCCA*	Cruz et al., 1985
PIIIA	ZRLCCGFOKSCRSRQCKO-HRCC*	Shon et al., 1988
SmIIIA	ZRCCNGRRGCSSRWCRDHSRCC*	West et al., 2002
SIIIA	ZNCCNG--GCSSKWCRDHARCC*	Bulaj et al., 2005
KIIIA	CCN----CSSKWCRDHSRCC*	Bulaj et al., 2005

Z, pyroglutamate; O, hydroxyproline; *, amidated C-terminal.

Materials and Methods

TIIIA Sequence by PCR. cDNA suitable for the production of either 5′ or 3′rapid amplification of cDNA ends PCR was manufactured from *C. tulipa* venom duct poly(A) mRNA using polymerase extension from a Not1-dt(18)-ANCHOR primer. This single-stranded cDNA was converted to double–stranded cDNA using RNAase-H/DNase-1 method, blunt ended, and ligated with Marathon (Clontech, Mountain View, CA) adaptors to both the 5′ and 3′ ends of the cDNA templates. A PCR assay capable of identifying μ-conopeptides was based on the PCR primers *Mu1A* plus *ANCHOR*. The *Mu1A* primer (5′-ATGATGTCTAAACTGGGAGTCTTG-3′) was based upon a comparison of nucleotide sequences from six different activity groups and considered specific for μ-conotoxins and related peptides.

Peptide Synthesis. μ-Conotoxin TIIIA and analogs were assembled manually with Boc SPPS chemistry (Schnölzer et al., 1992) using methods described previously (Nielsen et al., 2002). The side chain protections chosen were Arg(Tos), Lys(CIZ), Ser(Bzl) and Cys(p-MeBzl). The crude reduced peptides were purified by preparative chromatography, using a 1% gradient (100% A to 80% B, 80 min) and UV detection at 230 nm. Peptides were oxidized at 0.02 mM in either aqueous 0.33 M NH_4OAc/0.5 M GnHCl or 2 M NH_4OH/0.1 NH_4OAc at pH 7.8, 4°C in the presence of both reduced and oxidized glutathione (peptide/GSH/GSSG, 1:100:10 molar ratio). Oxidized peptides were purified by preparative RP-HPLC. TIIIA was quantified initially by triplicate amino acid analysis to produce an external reference standard for RP-HPLC (HP 1100) quantitation of each peptide. Mass spectra were acquired on a PerkinElmerSciex Instruments (Boston, MA) API III triple-quadrupole electrospray mass spectrometer (MS) in positive ion mode over *m/z* 500 to 2000 (0.1−0.2-Da steps, declustering potential 10−90 V, dwell time 0.4−1.0 s). Data were deconvoluted (MacSpec 3.2; MDS Sciex, Concord, ON, Canada) to obtain the molecular weight from the multiply charged species. MS was used to confirm purity and to monitor peptide oxidation. Synthetic TIIIA was used for subsequent characterization.

Radioligand Binding Studies. ^{125}I-TIIIA was prepared using 1,3,4,6-tetrachloro-3α,6α-diphenylglucoluril, stored at 4°C, and used within 4 weeks. ^{125}I-TIIIA was eluted after TIIIA on a Zorbax SB 300 C18 column (Agilent Technologies, Palo Alto, CA) as a broad peak on RP-HPLC, presumably because of the presence of monoiodinated His2 or His20. Unlabeled iodinated TIIIA (^{127}I-TIIIA) coeluted with ^{125}I-TIIIA and MS confirmed that the peak contained only monoiodinated species. Whole rat brain (Nielsen et al., 1999) and rat skeletal muscle (Yanagawa et al., 1988) were homogenized in 50 mM HEPES, pH 7.4, filtered though 100-μm nylon mesh (muscle only), and centrifuged at 28,000*g* (10 min). The pellet was suspended in 50 mM HEPES and 10 mM EDTA, pH 7.4, for 30 min, centrifuged, and resuspended in 50 mM HEPES, pH 7.4. Attempts to establish the ^{125}I-TIIIA and [^3H]STX assays using buffers compatible with both assays were unsuccessful, hence conditions for each assay are described separately. [^3H]STX displacement studies were performed in 130 mM choline chloride, 5.4 mM KCl, 5.5 mM glucose, 0.8 mM $MgSO_4$, 1.8 mM $CaCl_2$, and 50 mM HEPES, pH 7.4 with Tris base. ^{125}I-TIIIA displacement studies were performed in 20 mM HEPES, 75 mM NaCl, 0.2 mM EDTA, 0.2 mM EGTA, 0.5 units of aprotinin, 2 mM leupeptin, and 0.1% BSA at pH 7.2. Assays were performed on rat brain (10 μg of protein, 150-μl total volume) and muscle (50 μg of protein, 300-μl total volume) that contained labeled ligand [5.6 nM [^3H]STX at 14.9 Ci/mmol (Amersham, Little Chalfont, Buckinghamshire, UK) or 30 pM ^{125}I-TIIIA] and varying concentrations of μ-conotoxins, TTX, and STX in assay buffer. Assays were incubated for 1 h at 4°C or RT for ^{125}I-STX and ^{125}I-TIIIA, respectively. Membranes were then filtered through GFB filters (Whatman, Maidstone, UK) on a Tomtec (Hamden, CA) harvester (brain) or a Millipore (Billerica, MA) manifold (muscle) and washed with [^3H]STX wash buffer containing 163 mM choline chloride, 1.8 mM $CaCl_2$, 0.8 mM $MgSO_4$, and 5.0 mM HEPES, pH 7.4 with Tris base, or ^{125}I-

TIIIA wash buffer of 20 mM HEPES and 125 mM NaCl, pH 7.2. Filters used in ^{125}I-TIIIA assays were presoaked in 0.6% polyethyleneimine (PEI). Filters were dried, scintillant was added, and retained radioactivity measured on a Wallac Microbeta counter (PerkinElmer Life and Analytical Sciences, Boston, MA). Nonlinear regressions were fitted to triplicate data obtained for each experiment with Prism software (GraphPad, San Diego, CA). Initial experiments to identify native TIIIA used an ^{125}I-[2–22]TIIIA assay to guide the fractionation by reversed-phase HPLC of an extract of *Conus striatus* crude venom. The isolated μ-conotoxin TIIIA sequence corresponding to the pure active peptide confirmed the PCR-derived sequence and identified three post-translational modifications (Table 1).

Electrophysiological Experiments. Sensory neurons from rat dorsal root ganglia (DRG) were isolated as described previously, and depolarization-activated Na^+ currents were recorded using the whole-cell patch-clamp technique (Daly et al., 2004). Neurons were held at −70 mV in the whole-cell recording configuration and depolarized to 0 mV every 5 s. The current-voltage relationship was determined before and after toxin application. TTX-R Na^+ currents were recorded from small (<25 μm) neurons in the presence of 300 nM TTX, whereas TTX-S Na^+ currents were recorded from large (>25 μm) neurons that exhibited Na^+ currents with fast activation and inactivation kinetics and were inhibited to ≥95% of control current amplitude by TTX. When TTX-S Na^+ currents were studied, TTX was applied at the beginning of the experiment to determine the percentage of TTX-sensitive Na^+ current and washed out before application of μ-conotoxins.

Xenopus laevis oocytes were prepared as described previously (Fotia et al., 2004) and injected with capped RNA transcripts encoding subunits of rat $Na_v1.2$ (a gift from A. Goldin, University of California Irvine, Irvine, CA), rat $Na_v1.3$ (a gift from D. Ragsdale, McGill University, Montreal, QC, Canada), rat $Na_v1.4$ (gift from S. R. Levinson, University of Colorado, Denver, CO), human 1.5 (a gift from R. Kass, Columbia University, New York, NY), human $Na_v1.7$ (gift from N. Klugbauer and F. Hofmann, Teknishen Universität Munich, Munich, Germany), and human $Na_v1.8$ (cloned from human DRG tissue by PCR in our laboratory). The rat (r) $Na_v1.2$ was injected at 0.5 ng/oocyte and other subtypes at 2 ng/oocyte). Three days after cRNA injection, whole-cell Na^+ channel currents were recorded from oocytes using two-electrode (virtual ground circuit) voltage clamp technique, as described previously by Fotia et al., (2004). Selected μ-conotoxins were superfused at 3 μM for at least 10 min, and inhibition of TTX-R and TTX-S Na^+ current in DRG neurons and Na^+ current in oocytes expressing $Na_v1.2$, -1.3, -1.5, -1.7, or -1.8 was recorded. The potency of Na^+ current inhibition by TIIIA was determined at $Na_v1.2$ and $Na_v1.4$ coexpressed with rat β1 and rat β2 (gift from A.L. Goldin, University of California Irvine, Irvine, CA) in oocytes (1 ng of each injected).

^{1}H NMR Spectroscopy. All NMR experiments were recorded on a Bruker ARX 500 spectrometer equipped with a *z*-gradient unit or on a Bruker DMX 750 spectrometer equipped with a *x,y,z*-gradient unit. Peptide concentrations were ~2 mM. TIIIA was examined in 95% H_2O/5% D_2O, pH 3.0 and 5.5; 275–298 K, and in 100% D_2O. ^{1}H NMR experiments recorded were NOESY (Jeener et al., 1979; Kumar et al., 1980) with mixing times of 150, 200, and 400 ms and total correlation spectroscopy (Bax and Davis, 1985) with a mixing time of 80 ms, double quantum-filtered COSY (Rance et al., 1983), and exclusive COSY in 100% D_2O (Greisinger et al., 1987). All spectra were run over 6024 Hz (500 MHz) or 8192 Hz (750 MHz) with 4000 data points, 400 to 512 free induction decays, 16 to 64 scans, and a recycle delay of 1 s. The solvent was suppressed using the WATERGATE sequence (Piotto et al., 1992). Slow exchanging amides were analyzed by dissolving the peptide in D_2O followed by recording a series of one-dimensional and total correlation spectra. Amides still present after 24 h were classified as slow exchanging. When the exchange was complete, exclusive COSY and NOESY spectra were recorded. Spectra were processed using UXNMR (Bruker, Newark, DE) as described previously (Nielsen et al., 1999) and using Aurelia, subtraction of background was used to minimize T_1 noise. Chemical shift values of TIIIA and analogs were obtained in 95% H_2O/5% D_2O at 275 K and referenced internally to DSS at 0.00 ppm. Secondary Hα shifts were measured using random coil shift values of Wishart et al. (1995). $^3J_{NH\text{-}H\alpha}$ coupling constants were measured as described previously (Nielsen et al., 1999).

Distance Restraints and Structure Calculations. Peak volumes in NOESY spectra were classified as strong, medium, weak, or very weak corresponding to upper bounds on interproton distance of 2.7, 3.5, 5.0, or 6.0 Å, respectively. Lower distance bounds were set to 1.8 Å. Appropriate pseudoatom corrections were made according to Wüthrich et al. (1983), and distances of 0.5 Å and 2.0 Å were added to the upper limits of restraints involving methyl and phenyl protons, respectively. Appropriate restraints for the three disulfide bonds (Cys4–Cys16, Cys5–Cys21, and Cys11–Cys22) were included in the calculations. $^3J_{NH\text{-}H\alpha}$ coupling constants were used to determine ϕ dihedral angle restraints (Pardi et al., 1984) with $^3J_{NH\text{-}H\alpha}$ coupling constants ≤6 Hz or ≥8 Hz corresponding to a dihedral angle of −65 ± 30° and −120 ± 40°, respectively. In cases where $^3J_{NH\text{-}H\alpha}$ was 6 to 8 Hz and it was clear that a positive dihedral angle was not present, ϕ was restrained to −100 ± 70°. $^3J_{H\alpha\text{-}H\beta}$ coupling constants gathered from the ECOSY, together with relevant NOESY peak strengths, were used to determine χ1 dihedral angle restraints. Where there was no diastereospecific assignment for a prochiral pair of protons, the largest upper bound for the two restraints was used. Where stereospecific assignments were established, these distances were specified explicitly.

A total of 473 NOE-derived distance restraints (166 intraresidue, 137 sequential, 170 long/medium range) and 21 dihedral angle restraints (13 ϕ and 8 χ1) were used to generate a set of 50 structures of TIIIA. Structures were calculated using the torsion angle dynamics/simulated annealing protocol in X-PLOR (Brünger, 1992) version 3.8 using a modified geometric forcefield based on parhdg.pro. Of the 50 structures initially generated, 49 were chosen for further refinement. Structural refinements were performed using energy minimization (200 steps) under the influence of a full forcefield derived from Charmm (Brooks et al., 1983) parameters. Visualization and superimpositions of 20 structures with the lowest energies were done using Insight II (Accelrys, San Diego, CA). Surface calculations, RMSDs, and H-bond analysis were done using MOLMOL (Koradi et al., 1996). The quality of the structures was analyzed using procheck-NMR (Laskowski et al., 1998).

Results

Discovery of TIIIA. The *Mu1A* primer yielded a PCR product with a distinct band of DNA at ~800 bp as well as a band at ~400 bp. The 800-bp band was excised, purified, and cloned into PCR direct TA-plasmid vectors (Invitrogen, Carlsbad, CA), and white recombinant clones were randomly selected and amplified in overnight cultures. Plasmid DNA was extracted from each culture and used as templates for DNA sequencing. The *Mu1A* primer identified μ-conotoxin GIIIA from *Conus marmoreus, C. tulipa, Conus magus,* and *Conus geographus.* A single new peptide (that we named TIIIA) having the same cysteine framework as GIIIA and PIIIA was found in *C. tulipa* (Table 1). No other conotoxins with this cysteine framework and an arginine in loop II were identified. The derived amino acid sequence, including two predicted hydroxyproline residues and an amidated C terminus, revealed considerable sequence divergence from other μ-conotoxins. Excluding the conserved cysteine residues, TIIIA had 25% sequence identity with PIIIA, 29% sequence identity with GIIIA, 18% sequence identity with GIIIB, and 35% sequence identity with SmIIIA (Table 1).

TIIIA Isolation from Crude Venom. Given its detection in cDNA by PCR, native TIIIA was not detected in batches of crude venom obtained from *C. tulipa*. Instead, native TIIIA was isolated from a batch of crude venom of *C. striatus* using an ^{125}I-[2–22]TIIIA assay to guide fractionation, indicating that its production may be transcriptionally regulated. Sequencing of the isolated peptide confirmed the PCR-derived sequence, including the presence of Arg1, which was unexpectedly retained in native TIIIA (Table 1) and not cleaved at this site by endogenous processing proteases (Milne et al., 2003).

Radioligand Binding Studies. Synthetic μ-TIIIA displaced [^{3}H]STX from VGSCs in rat brain and rat skeletal muscle with similar potencies (Fig. 1). However, TIIIA was unable to fully displace [^{3}H]STX from rat brain, disclosing a TIIIA-resistant component of ~15%, equivalent to the resistant component remaining in the presence of PIIIA (Fig. 1D). ^{125}I-TIIIA labeled a single site in rat with nonspecific binding of ~10% at the K_d (Fig. 1A). Of the naturally occurring μ-conotoxins assayed, TIIIA had the highest affinity for neuronal VGSCs and was similarly potent to several other native μ-conotoxins at skeletal muscle VGSC (Fig. 1, Table 2). SAR analysis across the analogs revealed Arg14 to be the most critical residue for high-affinity interactions at both the neuronal and muscle subtypes, and this residue could not be substituted with alanine, glutamine or tyrosine (Fig. 2). Individual replacements of Lys6, Lys9, Arg17, or His20 with either Ala or Gln resulted in modest drops in potency, whereas a slight increase in potency at skeletal muscle VGSCs occurred when His2 and Gln19 were replaced with Ala. It is noteworthy that replacing Glu15 with Ala ([Ala15]-TIIIA) produced the highest affinity ligand known for both rat brain and muscle VGSCs. As expected for competitive inhibitors, all μ-conotoxin displacement curves had a Hill slope of ~−1.

Effects of TIIIA on Na^+ Currents in DRG. TIIIA and GIIIA were assessed for inhibition of TTX-R and TTX-S Na^+ currents in isolated DRG neurons. Neither toxin produced detectable block of the depolarization-activated Na^+ currents at 3 μM, nor did they affect the current-voltage relationship (data not shown).

Effects of μ-Conotoxins on Oocyte-Expressed VGSC Subtypes. The μ-conotoxins GIIIA, GIIIB, PIIIA, and TIIIA were assessed for inhibition of VGSC subtypes expressed in *X. laevis* oocytes (Fig. 3). TIIIA at 3 μM inhibited $rNa_v1.2$ to ~95% but was inactive at the other VGSC subtypes tested (Fig. 3A). This effect was reversed upon washout for ~30 min. TIIIA inhibited $rNa_v1.2$ current with an IC_{50} of 40 nM (pIC_{50}, 7.4 ± 0.04 M) and $rNa_v1.4$ current with an IC_{50} of 9 nM (pIC_{50}, 8.0 ± 0.09 M). PIIIA at 3 μM also completely inhibited the inward Na^+ current mediated by $rNa_v1.2$ and caused a small (~30%) inhibition of $hNa_v1.7$ but did not affect the other VGSC subtypes tested in this study (Fig. 3B). The block of $rNa_v1.2$ by PIIIA was slowly reversible, whereas the inhibition of $hNa_v1.7$ was completely reversed upon washout for 30 min. We were surprised to find that GIIIB at 3 μM almost completely abolished $rNa_v1.2$ current and inhibited ~50% of $rNa_v1.3$-mediated Na^+ current. GIIIB also caused a small inhibition of $hNa_v1.5$ but was without effect on $hNa_v1.7$ or $hNa_v1.8$ (Fig. 3C). The block of VGSCs by GIIIB was reversed upon washout for ~15 min. GIIIA at 3 μM did not affect any of the neuronal VGSC subtypes exam-

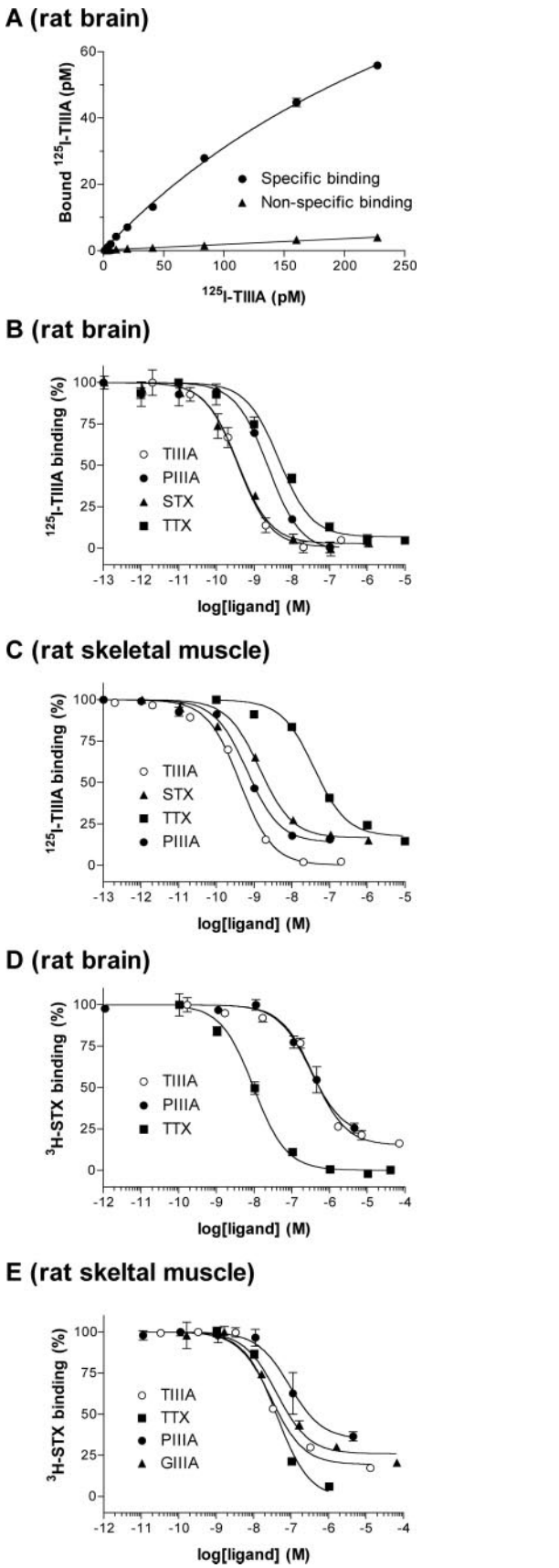

Fig. 1. Displacement of site 1 toxins from VGSCs. A, saturation binding curve for ^{125}I-TIIIA on rat brain VGSCs. Displacement of ^{125}I-TIIIA from rat brain (B) and rat skeletal muscle VGSCs (C). Displacement of [^{3}H]STX from rat brain (D) and rat skeletal muscle VGSC (E).

ined (data not shown), consistent with its selectivity for muscle-type VGSCs demonstrated previously (Cruz et al., 1985). In addition, SmIIIA was also assessed for inhibition of $hNa_v1.8$ because this toxin has previously been shown to inhibit TTX-R VGSCs in amphibian sympathetic and DRG neurons (West et al., 2002). SmIIIA at 3 μM did not inhibit $hNa_v1.8$ (data not shown) indicating that SmIIIA is active at amphibian but not human TTX-R VGSCs.

^{1}H NMR Spectroscopy. The ^{1}H NMR spectra of μ-conotoxins have historically been difficult to interpret because they exhibit broadened lines indicative of conformational exchange among distinct conformations as a result of *cis*/*trans* isomerization of a hydroxyproline (Hyp) in loop 1. As a result, the constraints derived from this less definitive NMR data have not resulted in well defined 3D structures. In contrast, the ^{1}H NMR spectra of TIIIA and its analogs show no evidence of conformational exchange in solution; instead, they produce narrow and well dispersed peaks and well defined NOEs. In support, both Hyp8 and Hyp18 of TIIIA show strong sequential Hδ-Hα_{i-1} NOEs, indicating that they exist in the *trans* conformation. No evidence for the *cis* conformation of TIIIA was found.

To identify any structural effects of residue replacements on the backbone conformation of TIIIA measurements of secondary Hα chemical shifts, Hβ shifts and $^3J_{NH\text{-}H\alpha}$ couplings were measured for each of the TIIIA analogs. All analogs of TIIIA had similar values, indicating they have the same overall fold and a high retention of backbone and side-chain structural integrity across the set of peptides. This is exemplified by the conservation of secondary Hα shifts, indicating no differences in backbone conformation among TIIIA, [2–22]TIIIA and Ala-substituted (Fig. 4A) or Gln-substituted (Fig. 4B) TIIIA. Minor differences in secondary Hα backbone chemical shifts were seen for His2 and for Gly7 and Gly10. Small local changes were also observed for [Ala17]TIIIA, [Ala19]TIIIA, [Gln2]TIIIA and [Gln20]TIIIA around the site of the substitution. None of the analogs exhibited spectra indicative of conformational exchange between multiple conformations, indicating that the TIIIA scaffold is resilient to single residue changes. The three-dimensional structure of TIIIA is described below.

3D Structure of TIIIA. Of the 50 structures generated, 49 converged to a similar fold with no NOE violations greater than 0.2 Å and no dihedral violations greater than 3°. These 49 structures were subjected to further refinement (see *Materials and Methods*) and the 20 lowest energy structures chosen for final structural analysis. Comparison of these structures revealed that the backbone structure of TIIIA was highly defined over residues 3 to 22, as evidenced by high average angular order parameters (S = 0.97) over this region for the ϕ and ψ backbone dihedral angles and the low backbone RMSD (Fig. 5). The local medium-range NMR data that provide information on the secondary structure of TIIIA are given in Fig. 6. The presence of several Hα-NH_{i+2} and Hα-NH_{i+3} NOEs suggests that several turns are present across the peptide, and despite the presence of several long-range NOEs, there was no evidence in TIIIA of the β-hairpin identified in GIIIB (Hill et al., 1996). Superimposition of the 20 lowest energy structures (Fig. 7) revealed the existence of a well ordered central region dominated by a series of turns, with some disorder present at the N-terminal tail. Like SmIIIA (Keizer et al., 2003), TIIIA showed signs of a distorted 3_{10}-helix across residues 12 to 15, including the pres-

TABLE 2

μ-Conotoxin and TTX potency (pIC_{50} ± S.E.) to displace [^{3}H]STX or ^{125}I-TIIIA binding to rat brain and rat muscle membrane

Data are means of three to seven separate experiments.

μ-Conotoxin	Rat Brain		Rat Muscle	
	[^{3}H]STX	^{125}I-TIIIA	[^{3}H]STX	^{125}I-TIIIA
TIIIA	7.8 ± 0.1	9.2 ± 0.2	7.8 ± 0.1	9.7 ± 0.3
[A15]TIIIA	N.D.	10.2 ± 0.1	N.D.	10.1 ± 0.1
PIIIA	6.5 ± 0.2	8.7 ± 0.1	6.9 ± 0.1	9.1 ± 0.1
GIIIA	4.6 ± 0.2	6.5 ± 0.4	7.5 ± 0.1	9.8 ± 0.1
GIIIB	5.8 ± 0.2	7.9 ± 0.2	7.8 ± 0.3	9.9 ± 0.1
GIIIC	<5	6.3 ± 0.2	7.5 ± 0.1	9.8 ± 0.1
TTX	8.2 ± 0.1	8.3 ± 0.2	7.7 ± 0.1	7.3 ± 0.5

N.D., not determined.

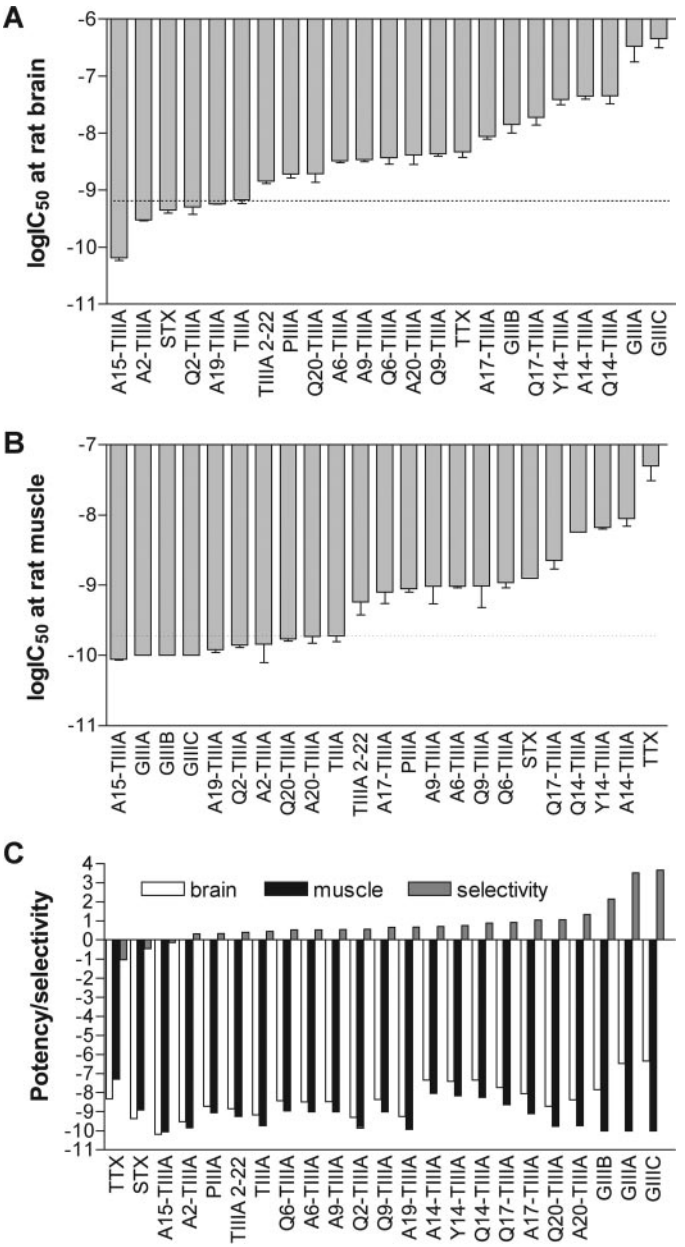

Fig. 2. Potency and selectivity of TIIIA and analogs at rat brain (A) and rat skeletal muscle (B). C, neuronal versus muscle selectivity is ordered from the most neuronally selective ligand (TTX). Potency is the IC_{50} (M) values for displacement of ^{125}I-TIIIA (mean ± S.E.M.).

ence of small $^3J_{HN\text{-}H\alpha}$ coupling constants and several i, $i+3$ NOEs in this region (Fig. 6).

Analysis of the TIIIA surface area revealed that Ser13 is relatively buried in the molecule in a manner that promotes greater exposure of Arg14 (Fig. 8), as seen previously for PIIIA (Nielsen et al., 2002), Replacing Glu15 with the smaller Ala in [Ala15]-TIIIA may further promote Arg14 exposure, perhaps contributing to the enhanced affinity observed on removal of the glutamic acid. Aside from Glu15, most of the polar and hydrophilic residues are surface-exposed, including Arg1, His2, Lys6, Hyp8, Lys9, Arg17, Hyp18, and His20, which in the 3D structures are spread across the molecule. The SAR analysis of TIIIA revealed that with the exception of His2, all of the exposed basic residues identified in the structure contributed at least modestly to the activity of TIIIA at both neuronal and skeletal VGSCs.

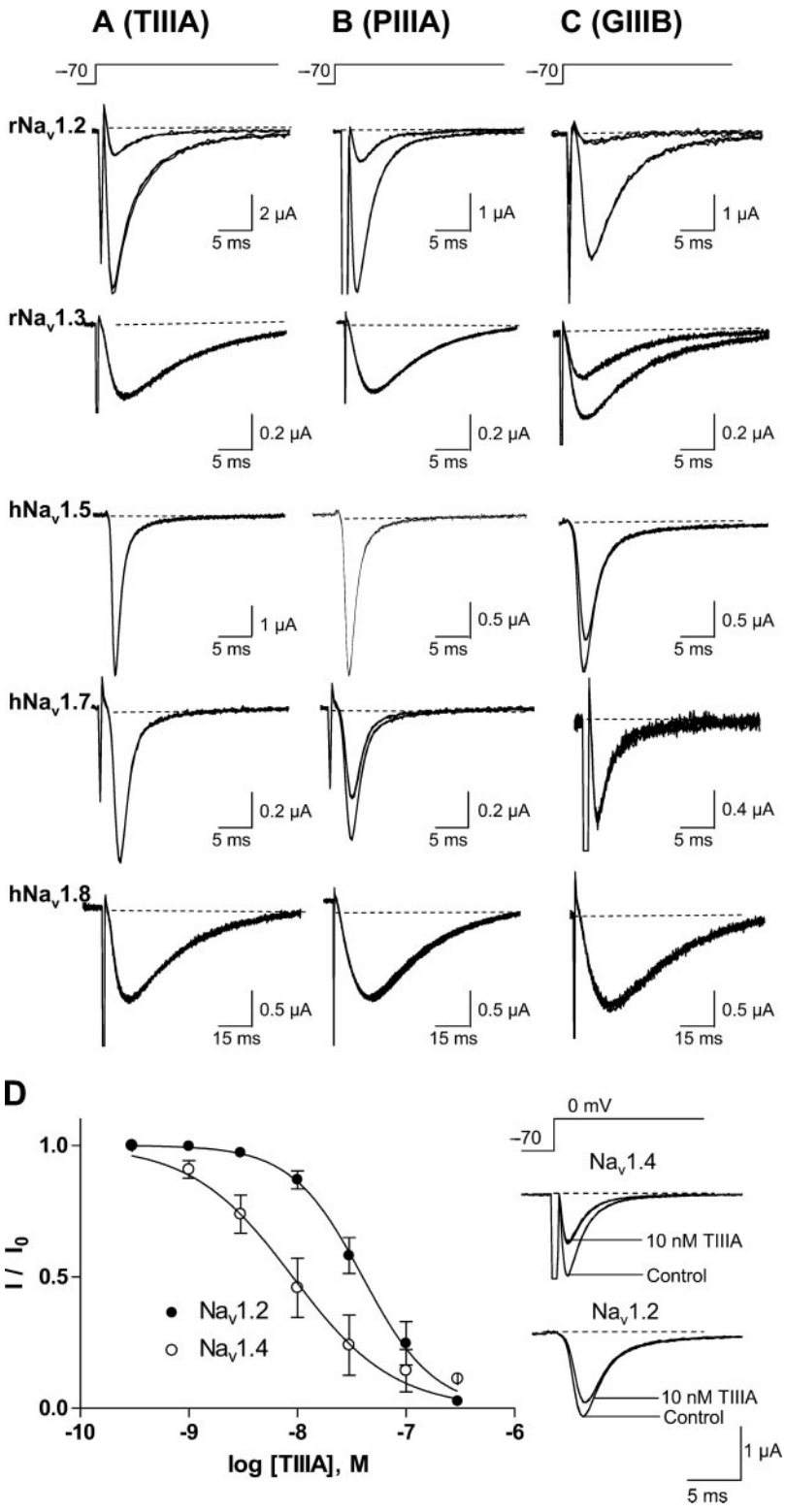

Fig. 3. Effects of μ-conotoxins on different neuronal Na_v expressed in oocytes. Superimposed Na^+ current through $Na_v1.2$, -1.3, -1.5, -1.7, and -1.8 before and after addition of 3 μM TIIIA (A), PIIIA (B), and GIIIB (C) are shown (single traces indicate no observable change in current). D, concentration-response relationships for TIIIA inhibition of Na^+ currents mediated by $Na_v1.2$ (IC_{50} 40 nM) and $Na_v1.4$ (IC_{50} 9 nM). Superimposed inward Na^+ currents evoked by a voltage step to 0 mV from a holding potential of −70 mV are shown in the absence (control) and presence of 10 nM TIIIA for $Na_v1.4$ and $Na_v1.2$.

These activity data are consistent with TIIIA binding to neuronal and skeletal VGSCs in a similar manner. Furthermore, the overlap between structure and activity supports the view that the 3D structure of TIIIA is the μ-conotoxin conformation that binds to VGSCs.

Discussion

This study reports the isolation and characterization of μ-conotoxin TIIIA. The sequence of TIIIA was initially determined by PCR amplification and cloning of *C. tulipa* venom duct cDNA, and the sequence was confirmed by assay-guided fractionation of crude *C. striatus* venom. Synthetic TIIIA at low nanomolar concentrations displaced [^{3}H]STX binding to both rat muscle and nerve TTX-S sodium channels. A residual component of [^{3}H]STX binding (~15%) was not displaced by TIIIA, suggesting it discriminates among native TTX-S VGSC subtypes found in rat brain.

Given the high affinity of TIIIA for TTX-S Na^+ channels in rat brain, it was somewhat surprising that TIIIA was without effect on the TTX-S Na^+ current in DRG. Rat DRG neurons express $Na_v1.1$, Na_v 1.6, $Na_v1.7$ (Schaller et al., 1995; Felts et al., 1997; Toledo-Aral et al., 1997), and $Na_v1.3$ in neuropathic pain states (Black et al., 1999). Using a *X. laevis* oocyte expression system, we confirmed that TIIIA was without effect on depolarization-activated Na^+ current from TTX-S $Na_v1.3$ and -1.7 and TTX-R $Na_v1.5$ and -1.8. In contrast, TIIIA potently inhibited Na^+ current through $Na_v1.2$ (and $Na_v1.4$). This inhibition occurred without otherwise affecting the I-V relationship for the VGSC. Thus μ-conotoxin TIIIA is selective for the dominant VGSC subtype present in the brain ($Na_v1.2$) and not TTX-S channels expressed in DRG neurons. Lack of detectable inhibitory activity in rat DRG neurons confirms that significant levels of $Na_v1.2$ are not expressed in adult DRG neurons (Black et al., 1996). The incomplete inhibition of [^{3}H]STX binding in rat brain produced by TIIIA is consistent with a selective effect on $Na_v1.2$ over other brain VGSCs, including $Na_v1.1$.

To examine selectivity differences among the known μ-conotoxins, we also determined VGSC subtype selectivity for PIIIA, GIIIA and GIIIB. The previously reported selectivity of PIIIA ($Na_v1.2 > Na_v1.7$) was confirmed in the present study. PIIIA inhibits the TTX-S Na^+ current in rat DRG neurons (Shon et al., 1998; Nielsen et al., 2002), consistent with an ability to inhibit $Na_v1.7$. GIIIB, previously consid-

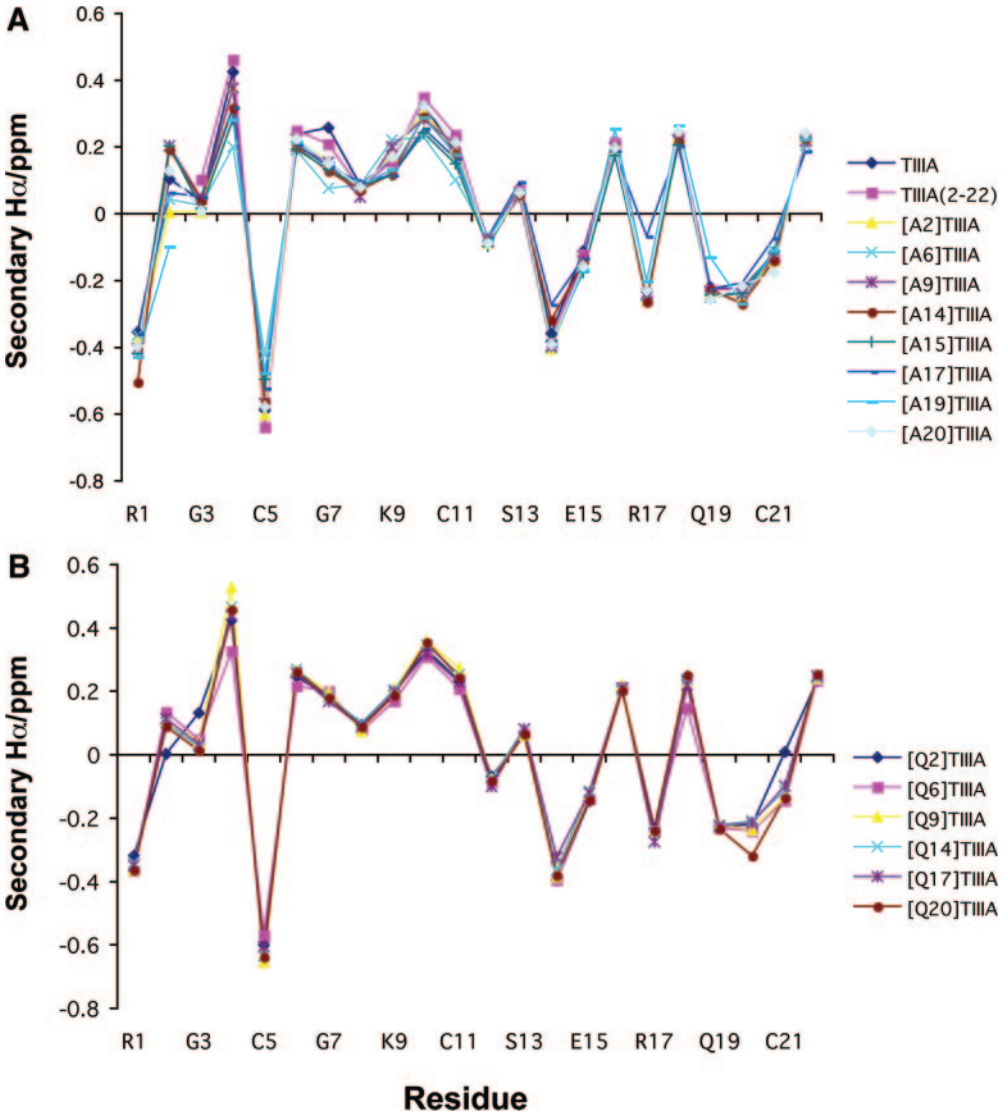

Fig. 4. Secondary Hα shifts of TIIIA and analogs. A, TIIIA compared with TIIIA(2−22) and Ala-substituted analogs. B, comparison of TIIIA and Gln-substituted analogs.

ered be selective for $Na_v1.4$ (Hill et al., 1996), also inhibited $Na_v1.2$, $Na_v1.3$, and, to a lesser extent, $Na_v1.5$. GIIIB differs from both GIIIA and GIIIC at only two positions, indicating that at least one of these residues has an important effect on VGSC subtype selectivity. The lack of effect of μ-conotoxins on $Na_v1.8$ is in contrast to the action of μ-conotoxins that preferentially target this VGSC subtype and produce an antinociceptive effect when administered intrathecally in animals (Ekberg et al., 2006).

A high-resolution 3D NMR structure of TIIIA was determined and is compared with the published structures of GIIIB (Hill et al., 1996), PIIIA (Nielsen et al., 2002), and SmIIIA (Keizer et al., 2003) in Fig. 9. This comparison reveals a similar overall global structure as well as a number of structural differences among the μ-conotoxins. Although GIIIB has a short stretch of distorted α-helix and an antiparallel β-sheet joined by a β-hairpin, the major conformation of TIIIA, like PIIIA and SmIIIA, contained no β-sheet region and instead comprised several well defined turns. In addition, the spectra of TIIIA indicated that only a single conformation existed in solution. In contrast, PIIIA occurred as two distinct conformations in a 3:1 ratio. These PIIIA conformations arose from *cis*/*trans* isomerisation at Hyp8, with the minor conformation resembling the N-terminal part of GIIIA and GIIIB, which have a *cis* Hyp in loop 1 (Nielsen et al., 2002) and broadened lines indicative of conformational exchange (Hill et al., 1996). In contrast, both Hyp residues in TIIIA are found in the *trans*-conformation, and no interchange between the *trans* and *cis* states was observed. It is noteworthy that the recently reported SmIIIA structure also adopts a single conformation (Keizer et al., 2003) that was attributed to the absence of Hyp in the peptide. Given the well defined nature of the TIIIA structure and its resilience to substitution, combined with the inability to adopt a *cis* conformation, we propose that μ-conotoxins bind to VGSCs in the *trans* confirmation originally identified in PIIIA (Nielsen et al., 2002). The extent to which these structures differ from the structure of TIIIA that binds to the VGSC remains to be determined.

Overlaying the structure of GIIIA, GIIIB, PIIIA, and SmIIIA (Ott et al., 1991; Hill et al., 1996; Nielsen et al., 2002; Keizer et al., 2003) with TIIIA, it is evident they share a similar backbone conformation over the C-terminal region

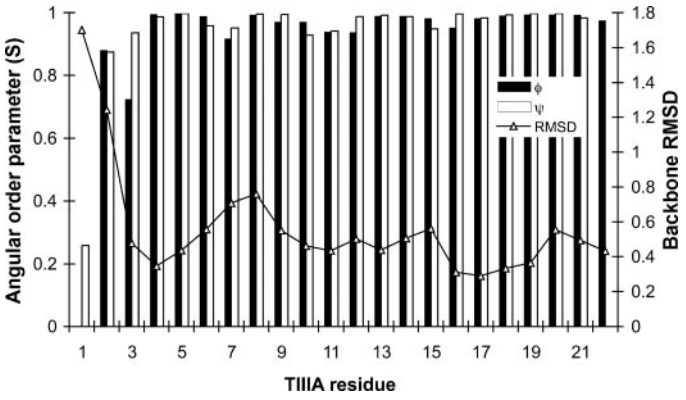

Fig. 5. Backbone angular order parameters (S) for the φ and ψ dihedral angles for TIIIA and average backbone RMSDs versus TIIIA residue number.

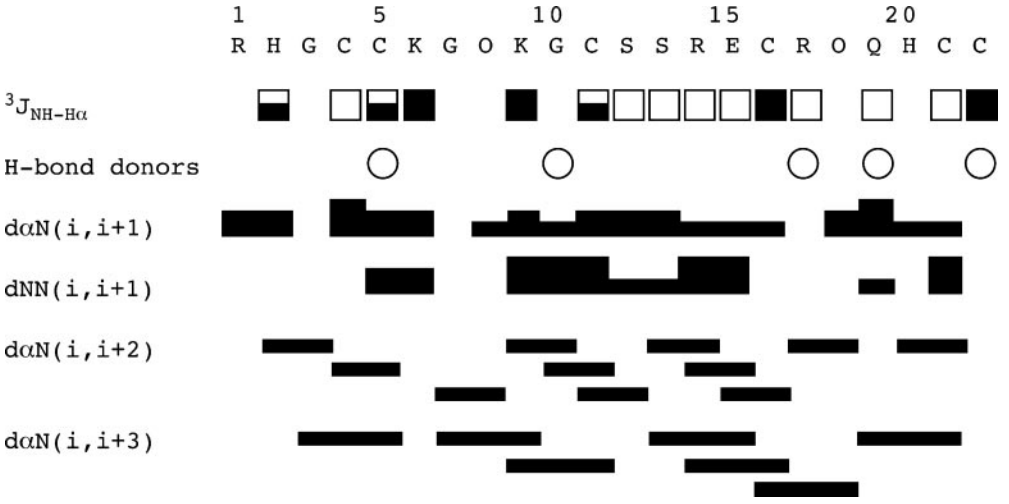

Fig. 6. Summary of local and medium range NOE, $^3J_{NH\text{-}H\alpha}$ coupling constants and slow exchange data for TIIIA (283 K, 100% D_2O, pH 3.5). ○, NH protons present 2 h after addition of D_2O; □, $^3J_{NH\text{-}H\alpha} \leq 6$ Hz; ■, $^3J_{NH\text{-}H_\alpha} \geq 8$ Hz; half-filled squares, 6 Hz $< {}^3J_{NH\text{-}H_\alpha} < 8$ Hz. For NOE data, height of bars indicate NOE intensity.

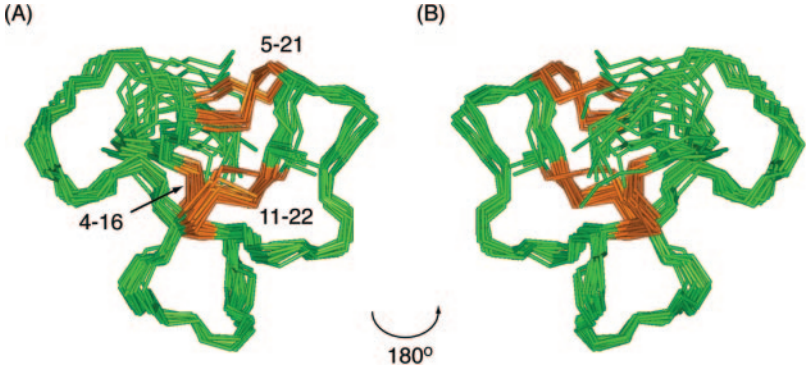

Fig. 7. Structure of TIIIA. A, backbone superimposition over the region 3 to 22 for the 20 lowest energy structures. B, 180$_y$° rotation of the structures shown in A, with the disulfide bridges indicated in orange.

despite significant sequence divergence. Superimposing the C-terminal region (12–22) of TIIIA with PIIIA (12–22), GIIIA (11–21), GIIIB (11–21), and SmIIIA (11–21) gave RMSD values of 0.65, 0.77, 0.70, and 1.88, respectively, confirming their structural similarity. The relatively high RMSD values for SmIIIA compared with TIIIA across the C-terminal region presumably arise from the extra residue in loop 4 of SmIIIA (Keizer et al., 2003). Superimposing TIIIA across the ordered region of PIIIA (4–22), GIIIA, GIIIB and SmIIIA (3–21) gave RMSDs of 1.32, 1.70, 1.87, and 2.22, respectively. These higher RMSD values reflect greater disorder in this region as well as distinct N-terminal conformations. For GIIIA and GIIIB, this can be attributed to the *cis*-conformation of Hyp7 giving rise to a β-hairpin that is not present in the major conformation of PIIIA or the single conformations of TIIIA and SmIIIA.

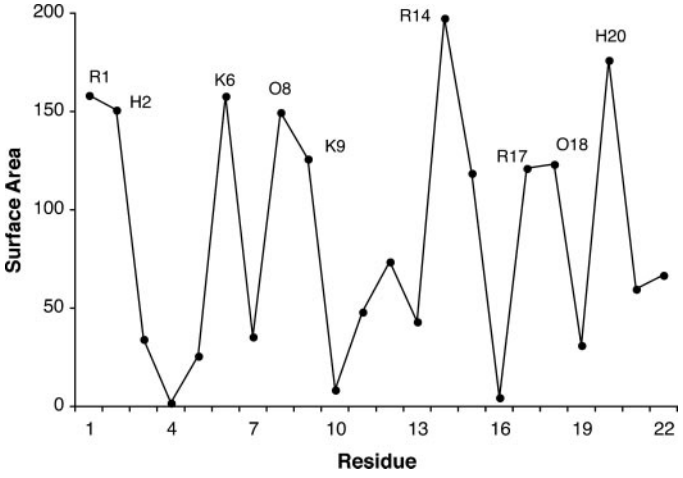

Fig. 8. Surface area of TIIIA as calculated in Insight II highlighting the exposed charged residues including Lys6, Lys9, Arg14, Arg17, and His20.

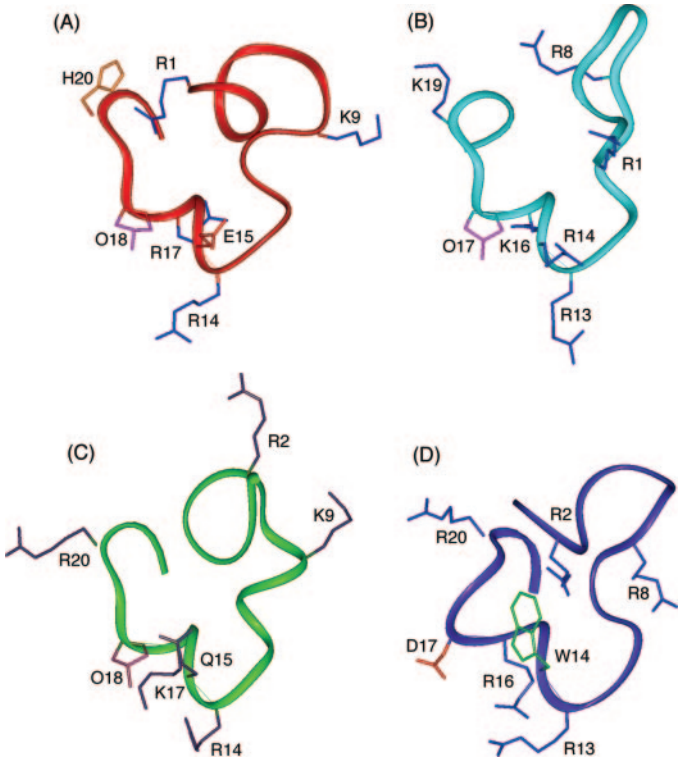

Fig. 9. Ribbon representation of μ-conotoxin TIIIA in red (A), GIIIB in cyan (Hill et al., 1996; PBD code 1GIB) (B), PIIIA in green (Nielsen et al., 2002; PBD code 1R9I) (C), and SmIIIA in *purple* (Keizer et al., 2003; PBD code 1Q2J) (D). Peptide superimposed across the backbone residues 11 to 18 of TIIIA with the corresponding residues in PIIIA (11–18), GIIIA (10–17), and SmIIIA (10–17). A comparison of surface residues is shown with side chains colored: Arg/Lys/Gln, blue; Asp/Glu, red; Hyp, pink; Trp, green; and His, orange. Residues are numbered according to their individual primary sequence (see Table 1) highlighting the similarities and differences between peptides.

Previous structure-activity studies have identified Arg14 in PIIIA as the key residue contributing to binding at the skeletal muscle VGSC subtype (Shon et al., 1998). For GIIIA, the corresponding Arg13 is the most important residue for binding to the muscle VGSC (Sato et al., 1991; French et al., 1996). Other residues in GIIIA identified as contributing to interactions with $Na_v1.4$ are Arg1, Lys8, Lys9, Ly16, and Arg19 (Becker et al., 1992). Consistent with these earlier studies, replacing the exposed Arg14 in TIIIA with Ala, Tyr, or Gln resulted in the greatest decrease in potency at both muscle and neuronal VGSCs. The absence of secondary Hα chemical shift changes associated with replacement with Ala indicates an unaltered backbone conformation, confirming that the decrease in potency arises from the loss of a direct Arg14 binding interaction. Replacing the surface-exposed residues Lys6, Lys9, Arg17, or His20 with either Ala or Gln caused a modest reduction in affinity, whereas replacement of His2, Glu15, or Arg19 with Ala enhanced affinity. It is noteworthy that residues 6 and 9 are located on the side of the peptide opposite residues 14, 17, and 20, consistent with the view that μ-conotoxins use a broad surface area to occlude the pore of VGSCs. Again, these potency changes were not associated with NMR-detectable structural changes. Sato et al. (1991) previously observed that replacing non-Cys residues with either Ala or Lys in μ-conotoxin GIIIA did not significantly change secondary Hα-chemical shifts.

TIIIA has a negatively charged Glu15 adjacent to Arg14, whereas previously reported μ-conotoxins have either a Gln, Arg, or Trp residue in the corresponding position (see Table 1). Replacing Glu15 with Ala increased the binding affinity by 10-fold without affecting the backbone conformation, indicating that a negative charge in this position creates an unfavorable interaction with the sodium channel. It is noteworthy that [Ala15]-TIIIA was the only μ-conotoxin tested that was more selective for brain ($Na_v1.2$) over muscle ($Na_v1.4$) VGSCs. Replacing the relatively exposed His2 with an Ala also resulted in a small increase in affinity at brain VGSCs. Removing Arg1 ([2–22]TIIIA) did not alter the secondary Hα chemical shifts but did cause a slight drop in affinity at both rat brain and muscle VGSCs.

In conclusion, this study reports the isolation and characterization of TIIIA, a selective and potent probe for $Na_v1.2$ and Nav1.4. Residues critical to binding and selectivity of TIIIA at both $Na_v1.2$ and $Na_v1.4$ were identified and their relative positions on the structure of TIIIA determined. A mode of binding for TIIIA common to both $Na_v1.2$ and $Na_v1.4$ is proposed based on a comparison of μ-conotoxin structures. TIIIA provides a rigid structural template for guiding the development of improved pharmacophore models of the μ-conotoxin binding site on VGSCs and potentially new subtype-selective inhibitors. The ^{125}I-TIIIA binding assay established in this study provides a rapid and sensitive measure of Site 1 Na^+ channel activity that could replace [^{3}H]STX in binding assays for the detection of STX, TTX, and related

toxins contaminating seafood products. Given the relative ease of probe synthesis, fluorescently labeled TIIIA or [Ala15]-TIIIA might prove useful for assays and selectively marking the distribution of $Na_v1.2$ and 1.4 in nerve and muscle tissue.

References

Bax A and Davis DG (1985) MLEV-17 based two-dimensional homonuclear magnetization transfer spectroscopy. *J Magn Reson* **65:**355–360.

Becker S, Prusak-Sochaczewski E, Zamponi G, Beck-Sickinger AG, Gordon RD, and French RJ (1992) Action of derivatives of μ-conotoxin GIIIA on sodium channels. Single amino acid substitutions in the toxin separately affect association and dissociation rates. *Biochemistry* **31:**8229–8238.

Black JA, Cummins TR, Plumpton C, Chen YH, Hormuzdiar WN, Clare JJ, and Waxman SG (1999) Upregulation of a silent sodium channel after peripheral, but not central, nerve injury in DRG neurons. *J Neurophysiol* **82:**2776–2785.

Black JA, Dib-Hajj S, McNabola K, Jeste S, Rizzo MA, Kocsis JD, and Waxman SG (1996) Spinal sensory neurons express multiple sodium channel alpha-subunit mRNAs. *Brain Res Mol Brain Res* **43:**117–131.

Brooks B, Brucoli R, Olafson BO, States D, Swaminathan S, and Karplus M (1983) CHARMM: a program for macromolecular energy, minimization, and dynamics calculations. *J Comput Chem* **4:**187–217.

Brünger AT (1992) *X-PLOR Version 3.1. A System for X-ray Crystallography and NMR.* Yale University, New Haven, CT.

Bulaj G, West PJ, Garrett JE, Marsh M, Zhang M-M, Norton RS, Smith BJ, Yoshikami D, and Olivera BM (2005) Novel conotoxins from *Conus striatus* and *Conus kinoshitai* selectively block TTX-resistant sodium channels. *Biochemistry* **44:**7259–7265.

Catterall WA (2000) From ionic currents to molecular mechanisms: structure and function of voltage-gated sodium channels. *Neuron* **26:**13–25.

Catterall WA, Goldin AL, and Waxman SG (2005) International Union of Pharmacology. XLVII. Nomenclature and structure-function relationships of voltage-gated sodium channels. *Pharmacol Rev* **57:**397–409.

Cestele S and Catterall WA (2000) Molecular mechanisms of neurotoxin action on voltage-gated sodium channels. *Biochimie* **82:**883–892.

Chahine M, Chen L-Q, Fotouhi N, Walsky R, Fry D, Santarelli V, Horn R, and Kallen RG (1995) Characterizing the μ-conotoxin binding site on voltage-sensitive sodium channels with toxin analogs and channel mutations. *Receptors Channels* **3:**161–174.

Chang N, French RJ, Lipkind GM, Fozzard HA, and Dudley S Jr (1998) Predominant interactions between μ-conotoxin Arg-13 and the skeletal muscle Na^+ channel localized by mutant cycle analysis. *Biochemistry* **37:**4407–4419.

Cruz LJ, Gray WR, Olivera BM, Zeikus RD, Kerr L, Yoshikami D, and Moczydlowski E (1985) Conus geographus toxins that discriminate between neuronal and muscle sodium channels. *J Biol Chem* **260:**9280–9288.

Daly NL, Ekberg JA, Thomas L, Adams DJ, Lewis RJ, and Craik DJ (2004) Structures of μO-conotoxins from *Conus marmoreus*. Inhibitors of tetrodotoxin (TTX)-sensitive and TTX-resistant sodium channels in mammalian sensory neurons. *J Biol Chem* **279:**25774–25782.

Ekberg J, Jayamanne A, Vaughan CW, Aslan S, Thomas L, Mould J, Drinkwater R, Baker MD, Abrahamsen, B Wood JN, et al. (2006) μO-conotoxin MrVIB selectively blocks $Na_v1.8$ sensory neuron specific sodium channels and chronic pain without motor deficits. *Proc Natl Acad Sci USA* **103:**17030–17035.

Felts PA, Yokoyama S, Dib-Hajj S, Black JA, and Waxman SG (1997) Sodium channel α-subunit mRNAs I, II, III, NaG, Na6 and hNE (PN1): Different expression patterns in developing rat nervous system. *Brain Res Mol Brain Res* **45:**71–82.

Fotia AB, Ekberg J, Adams DJ, Cook DI, Poronnik P, and Kumar S (2004) Regulation of neuronal voltage-gated sodium channels by the ubiquitin-protein ligases Nedd4 and Nedd4–2. *J Biol Chem* **279:**28930–28931.

French RJ, Prusak-Sochaczewski E, Zamponi G, Becker S, Kularatna AS, and Horn R (1996) Interactions between a pore-blocking peptide and the voltage sensor of the sodium channel: An electrostatic approach to channel geometry. *Neuron* **16:**407–413.

George AL (2005) Inherited disorders of voltage-gated sodium channels. *J Clin Investig* **115:**1990–1999.

Goldin AL, Barchi RL, Caldwell JH, Hofmann F, Howe JR, Hunter JC, Kallen RG, Mandel G, Meisler MH, Netter YB, et al. (2000) Nomenclature of voltage-gated sodium channels. *Neuron* **28:**365–368.

Greisinger C, Sorenson OW, and Ernst RR (1987) Practical aspects of the E-COSY technique. Measurements of scalar spin-spin coupling constants in peptides. *J Magn Reson* **75:**474–492.

Hill JM, Alewood PF, and Craik DJ (1996) Three-dimensional solution structure of μ-conotoxin GIIIB, a specific blocker of skeletal muscle sodium channels. *Biochemistry* **35:**8824–8835.

Jeener J, Meier BH, Bachmann P, and Ernst RR (1979) Investigation of chemical exchange processes by two-dimensional NMR spectroscopy. *J Chem Phys* **71:**4546–4553.

Keizer DW, West PJ, Lee EF, Yoshikami D, Olivera BM, Bulaj G, and Norton RS (2003) Structural basis for tetrodotoxin-resistant sodium channel binding by μ-conotoxin SmIIIA. *J Biol Chem* **278:**26805–46813.

Koradi R, Billeter M, and Wüthrich K (1996) MOLMOL: A program for display and analysis of macromolecular structures. *J Mol Graph* **51:**29–32.

Kumar A, Ernst RR, and Wüthrich K (1980) A two-dimensional nuclear Overhauser enhancement (2D NOE) experiment for the elucidation of complete proton-proton cross-relaxation networks in biological macromolecules. *Biochem Biophys Res Commun* **95:**1–6.

Lancelin J-M, Kohda D, Tate S, Yanagawa Y, Abe T, Satake M, and Inagaki F (1991) Tertiary structure of conotoxin GIIIA in aqueous solution. *Biochemistry* **30:**6908–6916.

Laskowski RA, MacArthur MW, and Thornton JM (1998) Validation of protein models derived from experiment. *Curr Opin Struct Biol* **8:**631–639.

Milne TJ, Abbenante G, Tyndall JD, Halliday J, and Lewis RJ (2003) Isolation and characterization of a cone snail protease with homology to CRISP proteins of the pathogenesis-related protein superfamily. *J Biol Chem* **278:**31105–31110.

Nielsen KJ, Adams D, Thomas L, Bond TJ, Alewood PF, Craik DJ, and Lewis RJ (1999) Structure-activity relationships of ω-conotoxins MVIIA, MVIIC and 14 loop splice hybrids at N- and P/Q-type calcium channels. *J Mol Biol* **289:**1405–1421.

Nielsen KJ, Watson M, Adams DJ, Hammarström AK, Gage PW, Hill JM, Craik DJ, Thomas L, Adams D, Alewood PF, et al. (2002) Solution structure of μ-conotoxin PIIIA, a preferential inhibitor of persistent tetrodotoxin-sensitive sodium channels. *J Biol Chem* **277:**27247–27255.

Ott K-H, Becker S, Gordon RD, and Ruterjans H (1991) Solution-structure of μ-conotoxin GIIIA analysed by 2D-NMR and distance geometry calculations. *FEBS Lett* **278:**160–166.

Pardi A, Billeter M, and Wüthrich K (1984) Calibration of the angular dependence of the amide proton-Cα proton coupling constants, $^3J_{NH\alpha}$ in globular protein. *J Mol Biol* **180:**741–751.

Piotto M, Saudek V, and Sklenár V (1992) Gradient-tailored excitation for single-quantum NMR spectroscopy of aqueous solutions. *J Biomol NMR* **2:**661–665.

Rance M, Sørenson OW, Bodenhausen G, Wagner G, Ernst RR, and Wüthrich K (1983) Improved spectral resolution in cosy ^{1}H NMR spectra of proteins via double quantum filtering. *Biochem Biophys Res Commun* **177:**479–485.

Safo P, Rosenbaum T, Shcherbatko A, Choi DY, Han E, Toledo-Aral JJ, Olivera BM, Brehm P, and Mandel G (2000) Distinction among neuronal subtypes of voltage-activated sodium channels by μ-conotoxin PIIIA. *J Neurosci* **20:**76–80.

Sato K, Ishida Y, Wakamatsu K, Kato R, Honda H, Ohizumi Y, Nakamura H, Ohya M, Lancelin M, Kohda D, et al. (1991) Active site of μ-conotoxin GIIIA, a peptide blocker of muscle sodium channels. *J Biol Chem* **266:**16989–16991.

Schnölzer M, Alewood PF, Jones A, Alewood D, and Kent SBH (1992) In situ neutralization in Boc-chemistry solid phase peptide synthesis. *Int J Peptide Protein Res* **40:**180–193.

Schaller KL, Krezmien DM, Yarawsky PJ, Krueger BK, and Caldwell JH (1995) A novel, abundant sodium channel expressed in neurons and glia. *J Neurosci* **15:**3231–3242.

Shon K-J, Olivera BM, Watkins M, Jacobsen RB, Gray WR, Floresca CZ, Cruz J, Hillyard DR, Brink A, Terlau H, et al. (1998) μ-Conotoxin PIIIA, a new peptide for discriminating among TTX-sensitive Na channel subtypes. *J Neurosci* **18:**4473–4481.

Toledo-Aral JJ, Moss BL, Koszowski AG, Whisenand T, Levinson SR, Wolf JJ, Silos-Santiago I, Halegoua S, and Mandel G (1997) Identification of PN1, a predominant voltage-dependent sodium channel expressed principally in peripheral neurons. *Proc Natl Acad Sci USA* **94:**1527–1532.

West PJ, Bulaj G, Garrett JE, Olivera BM, and Yoshikami D (2002) μ-Conotoxin SmIIIA, a potent inhibitor of tetrodotoxin-resistant sodium channels in amphibian sympathetic and sensory neurons. *Biochemistry* **41:**15288–15393.

Wishart DS, Bigam CG, Yao J, Abildgaard F, Dyason HJ, Oldfield E, Markley JL, and Sykes BD (1995) ^{1}H, ^{13}C and ^{15}N random coil NMR chemical shifts of the common amino acids. Investigations of the nearest-neighbour effects. *J Biolmolec NMR* **5:**67–81.

Wood JN, Boorman JP, Okuse K, and Baker MD (2004) Voltage-gated sodium channels and pain pathways. *J Neurobiol* **61:**55–71.

Wüthrich K, Billeter M, and Braun W (1983) Pseudo structures for the 20 common amino acids for use in studies of protein conformations by measurements of intramolecular proton-proton distance constraints with nuclear magnetic resonance. *J Mol Biol* **169:**949–961.

Yanagawa Y, Abe T, Satake M, Odani S, Suzuki J, and Ishikawa K (1988) A novel sodium channel inhibitor from *Conus geographus*: purification, structure and pharmacological properties. *Biochemistry* **27:**6256–6262.

Address correspondence to: Richard J. Lewis, Institute for Molecular Bioscience, The University of Queensland, Brisbane, Qld 4072, Australia. E-mail: r.lewis@imb.uq.edu.au